



Parameter Optimization and Stability Analysis of Graphene Nanoscale Growth Process Based on Model Predictive Control

Junpeng Xie^{1,*}

¹ Shanghai 201210, China

SUMMARY: *In order to overcome the problems such as the complex interplay and dynamic evolution of multiple parameters (temperature, atmosphere, pressure, etc.) in the growth of graphene nanostructures that cannot be observed in real time, as well as the sluggishness of traditional empirical adjustment methods, the idea of optimizing the parameters during the growth process based on model predictive control is proposed. Taking chemical vapor deposition as an example, this paper establishes a computational control system with a framework of state variable representation, data modeling, rolling prediction, and closed-loop feedback, and incorporates temperature, CH₄ flow rate, H₂ flow rate, tank pressure, and surface growth state into the optimization model. The method is verified in the experimental device and simulation environment to achieve accurate tracking of the growth process, with the response lag time shortened to 0.74 s. The convergence time of the tracking reference signal is reduced to 2.31 s, ensuring a small steady-state error of 1.9% and good anti-disturbance recovery ability and stability. This study demonstrates that the online computer control strategy based on model predictive control can improve the parameter regulation efficiency and uniformity of the graphene nanostructure preparation process.*

Povzetek: Predlagana je MPC-zasnovana metoda optimizacije rasti grafenskih nanostruktur. Z računalniškim modeliranjem stanj, drsnim napovedovanjem in zaprtolančnim uravnavanjem izboljša odzivnost, konvergenco in stabilnost procesa ter ohrani robustno delovanje ob motnjah dosledno v simulacijah in laboratorijskih poskusih.

KEYWORDS: *Model Predictive Control; Graphene Nanoscale Structure; Parameter Optimization; Closed-loop Regulation*

1 Introduction

Graphene has been widely applied in flexible electronic products, micro-sensors, high-frequency devices, and new functional films due to its excellent carrier mobility, outstanding mechanical properties, and tunable interfaces. However, the key factor restricting its application is not the aforementioned excellent properties themselves, but whether stable and controllable high-quality reproducible preparation can be achieved. Although there is a relatively mature process route for preparing graphene by CVD method, there is a significant correlation among many factors such as temperature, reaction chamber pressure, CH₄/H₂ ratio, carrier gas flow rate, substrate surface condition, and internal field distribution of the reactor. The nucleation-growth-crystallization process shows dynamic and nonlinear characteristics. As a result, the entire preparation process is in a state of "difficult to ensure stability despite adjustable parameters" [1-3]. Existing studies have shown that the quality of graphene CVD

*kelvin4383@163.com

<https://doi.org/10.65102/is2026671>

products not only depends on the precursor concentration and reaction temperature, but is also greatly affected by the crystal orientation of the substrate. The addition method of H₂, reactor design, and local mass transfer conditions all play important roles. Even a slight deviation from reasonable parameters can lead to a series of problems such as abnormal initial nucleation density, non-uniform grain size, increased defects, and weakened non-uniformity of the film [4-7].

The research on the control strategies for graphene growth has gradually shifted from traditional empirical regulation to process engineering analysis and multi-factor comprehensive optimization. Yan et al. proposed a controllable graphene preparation based on process engineering design, stating that the growth mechanism should be understood from aspects such as reaction path design, characterization of reaction kinetics, and process synergy [8]. Meanwhile, Yan, Peng, and Tour clearly pointed out that to obtain high-quality single-crystal graphene, the key lies in achieving this delicate balance between nucleation and growth, rather than changes in a single parameter [9]. Kidambi et al. systematically discussed the parameter space on a polycrystalline copper substrate, indicating that the combined changes in temperature, hydrogen dilution degree, and carbon source input intensity would significantly alter the single-layer coverage and surface evolution state [10]. Papon et al. optimized CVD parameters using experimental design methods, proving that traditional statistical optimization can improve the growth effect to a certain extent, but such methods are more suitable for offline optimization and are difficult to cope with the dynamic fluctuations in the growth process [11]. Recent studies have extended the focus to the uniformity control of large-area graphene and the design of the internal flow field in the reactor, indicating that gas transport, thermal field distribution, and equipment configuration will directly affect the consistency of the growth results [12].

The development of in-situ monitoring and computer modeling has provided new technical conditions for the transition of graphene growth from "post-event characterization" to "in-process regulation". Tsakonas et al. conducted in-situ kinetic studies using reflection spectroscopy, proving that changes in the growth interface state can be reflected through online signals, providing a basis for real-time estimation of the reaction process [13]. Losurdo et al. and Zhang et al. analyzed the role of hydrogen in graphene growth, indicating that hydrogen not only affects the methane dehydrogenation process but also changes the adsorption, etching, and reconstruction behavior on the copper surface, thereby having a significant impact on the structural integrity and defect formation [14, 15]. Niu et al.'s research on the growth intermediates also demonstrated that there is a continuous correlation between carbon cluster evolution and defect graphene formation, meaning that the graphene growth process is not a completely "black box", but has a modellable, identifiable, and predictable foundation [16]. Popov et al. established an analytical model for Cu(111) surface graphene CVD growth, while Yang et al. used numerical simulation to analyze the influence of special flow channel structures on the growth behavior. These works enhanced the feasibility of process modeling from different perspectives [17, 18]. However, based on the current research results, most studies still mainly focus on mechanistic explanations, parameter statistics, experimental comparisons, or simulation analyses. There are still relatively few studies that truly integrate online perception, predictive computing, and closed-loop regulation as a whole.

From the perspective of control theory, the preparation of graphene nanostructures is a complex nonlinear system process with multiple inputs, dynamic constraints, and a lagging process; the rate of temperature increase or decrease is affected by the thermal inertia of the device and constraints such as pressure regulation of the airflow, and cannot be infinitely accelerated; the surface coverage, initial nucleation density, and defect concentration cannot simply be maintained in a stable state by a definite rule [19]. Among them, the Model

Predictive Control (MPC) method can better cope with this environment. Based on the predictive model, the system state at a future time point is estimated, and the optimal operation point is calculated under the premise of meeting the constraints, and the control sequence is iteratively updated and optimized in the next sampling period [20]. Compared with fixed threshold control, single-variable PID regulation, or offline parameter formulation, MPC is more suitable for handling process problems such as graphene growth that have multiple parameter interactions, multiple constraints in the objective function, and frequent disturbances. If combined with upper-level computer control systems, data acquisition modules, state estimation programs, and feedback execution units, a continuous closed-loop of "acquisition - prediction - optimization - feedback" can be formed in a computer environment, thereby advancing the growth regulation from static setting to dynamic optimization. To present more clearly the focus and limitations of the existing research, Table 1 summarizes the representative works in this field.

Table 1: Comparison of Existing Research on Control of Graphene Growth Parameters

Representative Study	Research Object	Main Method	Computer/Online Component	Focus	Main Limitation
Yan et al. [8]	Graphene CVD process engineering	Process route design and mechanism integration	Mainly based on offline analysis	Coordinated design of growth steps	Lacks online feedback control
Kidambi et al. [10]	Graphene growth on polycrystalline Cu	Experimental study of parameter space	Parameter statistics and result comparison	Effects of temperature and atmosphere conditions	Difficult to cope with time-varying disturbances
Tsakonas et al. [13]	In situ growth kinetics of graphene	In situ spectroscopic monitoring	Has real-time monitoring capability	Identification of kinetic parameters	No rolling optimization closed loop has been formed
Li et al. [12]	Uniformity of large-area graphene	Flow field and reactor analysis	Strong simulation capability	Factors affecting uniformity	Focuses more on offline simulation
Proposed Method	Entire growth process of graphene nanostructures	MPC + state modeling + feedback optimization	Real-time acquisition and rolling solution by host computer	Dynamic parameter optimization and stability analysis	High requirements for model accuracy and computational power

As shown in Table 1, the existing research has respectively touched upon key aspects such as process parameters, growth kinetics, reactor flow field, and online monitoring. However, there still has not been a truly unified closed-loop logic between material mechanism, process data and control decisions. A large number of studies have given parameter combinations before the experiment and evaluated the growth results after the experiment, lacking a real-time correction mechanism for dynamic deviations. Once there is a minor imbalance during the nucleation stage, the subsequent expansion process may amplify the error, ultimately resulting in discrete crystal domain sizes, insufficient continuity of the film layer, or an increase in the

defect rate. Therefore, how to couple the extraction of state variables in the graphene growth process, the update of prediction models, and the optimization of control quantities through the coupling of computer control systems has become a key issue for this field to move from "able to produce" to "able to stabilize control".

Based on this, this paper takes the growth process of graphene nanostructures as the research object and constructs a framework for dynamic parameter optimization and stability analysis based on model predictive control. Considering the evolution relationship of temperature, pressure, gas flow rate, and growth state variables, a computer real-time acquisition and feedback execution mechanism is introduced, and an integrated model for growth process state representation, rolling prediction, and closed-loop regulation is established. To answer this question, in this paper, we conducted a systematic analysis of the above methods from aspects such as model accuracy and sensitivity analysis, consistency test of observed values and simulation results, convergence speed analysis, robustness and comparison. This paper aims to address the following key issues: (1) Can an effective model be constructed to describe the key influencing factors in the process of preparing graphene, and can it also be used for online prediction? Secondly, can the MPC method adaptively adjust the growth path of graphene under the condition of multiple coupled factors? Thirdly, can the established feedback control scheme ensure its stability and convergence in the presence of disturbances? The research on these issues not only helps to improve the controllability and consistency of graphene nanostructures, but also provides a possible path for us to adjust the production of substances on the computer.

2 Construction of an Optimization Model for the Growth Process of Graphene Nanoscale Structures Based on Model Predictive Control

2.1 Analysis of the Mechanism of Graphene Nanoscale Structure Growth and Modeling Principles

The growth process of graphene nanoscale structures exhibits distinct multi-variable coupling characteristics. Its evolution is not determined solely by a single temperature or a single gas flow rate, but is influenced by the distribution of the thermal field, the decomposition rate of the precursor, the surface adsorption and desorption behavior, the migration of carbon active species, and the formation and edge expansion of nuclei. During the reaction process, even minor fluctuations in temperature, pressure, methane and hydrogen flow rates will change the carbon concentration on the substrate surface and the nucleation density, thereby affecting the grain size, coverage and defect level. Thus, the growth of graphene essentially belongs to a constrained, strongly time-varying, and weakly nonlinear dynamic process. Simply relying on fixed formulas or empirical tuning is difficult to maintain the stability control throughout the process.

Based on the above mechanism understanding, this paper follows the basic idea of "mechanism constraint - state expression - online prediction - closed-loop implementability" in model construction. The core of this is not to statically decompose the complex growth phenomenon, but to connect the physical process, data representation and control decision-making into a unified framework that can be iteratively updated through a computer control system. As shown in Figure 1, this paper divides the modeling process of graphene growth into five consecutive levels that are interconnected: the bottom layer focuses on the temperature field, pressure field and atmosphere changes in the CVD reaction chamber, the

upper layer acquires key process data through sensing and time synchronization, the upper computer completes the extraction of state variables, state space modeling and rolling prediction, and finally feeds the optimized results obtained from model predictive control back to the heating unit, flow controller and pressure regulation device to achieve real-time correction of growth parameters.

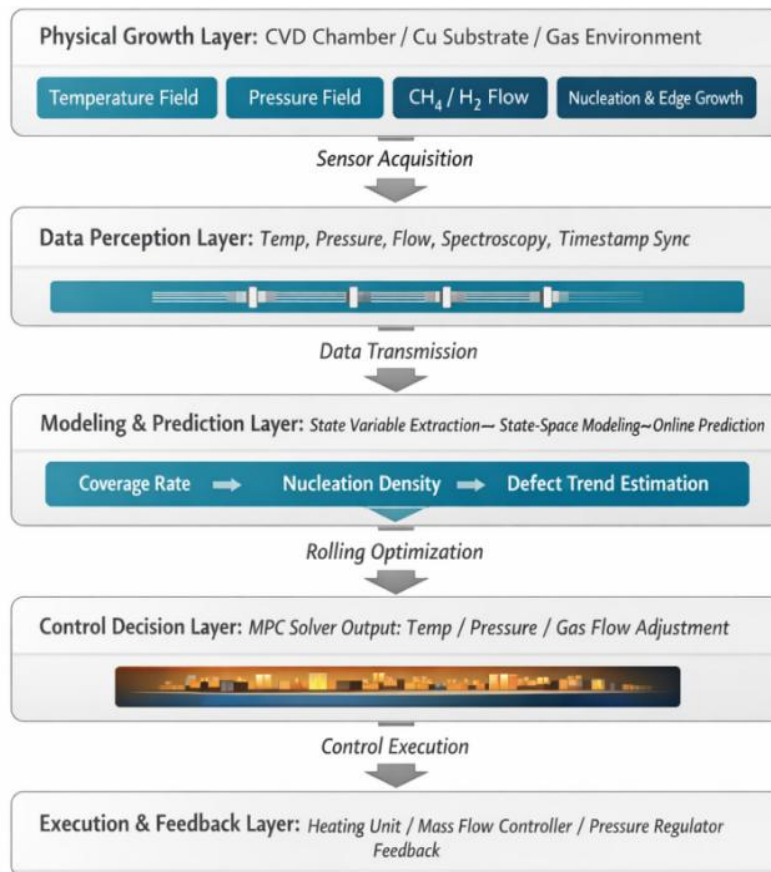


Figure 1: Graphene nanostructure growth mechanism - modeling - control mapping framework

Based on this, the model establishment needs to take into account both physical authenticity and computational feasibility. On one hand, key variables such as temperature, pressure, gas ratio, surface coverage and nucleation density should be extracted to ensure that the model can reflect the main dynamic relationships in the growth of graphene; on the other hand, redundant variables should be appropriately reduced to control the computational complexity, so that the model can meet the timeliness requirements of MPC online solution. The optimized model established according to this principle retains the key dynamic characteristics of graphene nanostructure growth and provides an executable mathematical basis for subsequent parameter dynamic optimization and stability analysis.

2.2 State Variable Characterization and Data Modeling Method for Growth Process

The growth process of graphene nanostructures exhibits characteristics such as continuous evolution, strong coupling of variables, and heterogeneous observation information. If a single process parameter is still used as the control basis, it is often difficult to accurately reflect the dynamic correlation between nucleation, expansion, and defect evolution. Therefore, in this

paper, temperature, pressure, and gas flow rate are not treated independently in the modeling process, but the process variables, surface state, and execution information are jointly included in the state characterization system. Through computer acquisition, time alignment, and feature mapping, a state space model that can be called for model prediction and control is constructed. The aim is not to stack the number of variables, but to obtain a compact state vector that can represent the growth trend, reflect the source of deviations, and support rolling optimization.

Based on the actual characteristics of the graphene CVD growth process, this paper defines the system input as heating power $u_T(t)$, methane flow rate $u_C(t)$, hydrogen flow rate $u_H(t)$, and cavity pressure adjustment quantity $u_P(t)$; the system state is represented by temperature $T(t)$, pressure $P(t)$, surface carbon concentration $C_s(t)$, nucleation density $N(t)$, coverage $G(t)$, and defect characterization quantity $D_f(t)$. The first two types of variables can be directly obtained by sensors, while the latter several types need to be indirectly estimated through spectroscopy, images, and historical process data. To ensure that the data enters the same calculation framework, a unified clock is set in the upper computer, and data with different sampling frequencies are resampled and timestamp-aligned to form a growth process observation set:

$$Z(t) = \{z_1(t), z_2(t), \dots, z_m(t)\} \quad (1)$$

Then, it is transformed into a state vector through the feature mapping function:

$$x(t) = f(Z(t)) = W\phi(Z(t)) + b \quad (2)$$

In this formula, W represents the feature mapping weight matrix, $\phi(\cdot)$ is the nonlinear feature extraction function, and b is the bias term. Here, a deep network structure is not adopted; instead, a shallow feature encoding method that is convenient for online updates is used to control the computational burden and ensure the real-time performance of subsequent MPC solution.

To enhance the specificity of state representation, this paper divides the main data sources and their modeling roles. The relevant content is shown in Table 2. Table 2 reflects the functional division of different acquisition nodes in the modeling of the growth process: temperature and pressure sensors are used to describe the underlying operating state, the feedback value of the mass flow controller mainly characterizes the input execution effect, in-situ spectral or image signals are used to supplement the surface coverage and defect change information, and control instructions and historical logs are used to reveal the temporal evolution characteristics and deviation propagation paths. The collaborative input of multi-source data enables the model to no longer remain at the level of single-point parameter monitoring, but can more completely depict the dynamic state of the graphene growth process.

Table 2: Main Data Sources and Modeling Parameter Settings during Growth Process

Data Source	Collected Content	Sampling Interval	Processing Method	Mapping Target
Temperature Sensor	Chamber temperature, heating rate	0.5 s	Filtering, interpolation	T(t)
Pressure Sensor	Reaction chamber pressure	0.5 s	Denoising, synchronization	P(t)
Mass Flow Controller	CH ₄ and H ₂ flow feedback	1 s	Normalization, encoding	Input vector u(t)
In situ spectroscopy/image module	Surface reflectance, coverage morphology	2 s	Feature extraction, dimensionality reduction	G(t), D _f (t)
Process logs and control commands	Setpoints, execution deviations, alarm records	1 s	Sequence encoding	State correction and error backtracking

After obtaining the state vector, the system also needs to characterize its evolution pattern over time. To achieve this, this paper employs a sliding time window to extract the feature of the state sequence. Let the window length be l , then the state trajectory matrix at time t is

$$X_t = [x(t-l+1), x(t-l+2), \dots, x(t)] \quad (3)$$

Based on this, the state increment is introduced to describe the changing trend of key variables:

$$\Delta x(t) = x(t) - x(t-1) \quad (4)$$

The significance of this treatment lies in the fact that the quality of graphene growth is not only determined by the absolute parameters at a certain moment, but is also closely related to the rate of parameter change and its cumulative effect. For instance, a short-term overshoot in temperature may not immediately alter the coverage rate, but will amplify the deviation in subsequent stages through changes in the concentration of active carbon and the nucleation rate. Incorporating incremental information into the state characterization makes the model more sensitive to dynamic anomalies and more suitable for predictive control's rolling correction.

Considering that some state quantities are obtained through indirect estimation, the model also needs to have an online error correction capability. In this paper, a deviation feedback mechanism for the predicted value and the observed value is set up in the upper computer. The error term is constructed by the observed state $x_m(t)$ at the current moment and the model estimated state $\hat{x}(t)$:

$$L_e = \|x_m(t) - \hat{x}(t)\|_2^2 \quad (5)$$

When the error exceeds the set threshold, the system invokes the recursive update strategy to correct the mapping parameters, thereby suppressing model drift and improving the accuracy of state mapping. As a result, data modeling is no longer a one-time offline fitting process, but a dynamic process that evolves synchronously with the actual growth process.

In summary, the state variable representation and data modeling method established in this section has completed the transformation from heterogeneous sensing information to a unified

state space, and has also incorporated computer acquisition, feature extraction, time series modeling, and error correction into the same framework. This method retains the key physical meanings in the growth of graphene nanostructures while controlling the model complexity, providing a reliable data foundation for subsequent MPC rolling optimization and closed-loop stability analysis.

2.3 Design of Dynamic Optimization Algorithm for Growth Parameters Based on Model Predictive Control

The parameter adjustment during the growth process of graphene nanostructures essentially belongs to a constrained multivariable dynamic optimization problem. The temperature, methane flow rate, hydrogen flow rate, and cavity pressure are not independent control variables; they are coupled and transmitted through the surface active carbon concentration, nucleation rate, and edge expansion speed. If fixed formulas or stage-based empirical tuning are still used, the control effect often depends on the operator's judgment and is difficult to adapt to the state deviations caused by thermal inertia, atmosphere fluctuations, and execution delays during the growth process. Based on this, this paper introduces the Model Predictive Control (MPC) algorithm into the upper computer control program, using the established state space model to conduct rolling predictions for the future limited time domain of the growth state, and re-solving the current control input in each sampling period, so that the parameter adjustment is transformed from static setting to dynamic optimization.

To balance growth quality and control stability, this paper writes the optimization objective as

$$J = \sum_{k=1}^{N_p} \|y(k|t) - y_{\text{ref}}(k)\|_Q^2 + \sum_{k=1}^{N_c} \|\Delta u(k|t)\|_R^2 \quad (6)$$

Among them, $y(k|t)$ represents the predicted value of the output at the next k steps from time t , $y_{\text{ref}}(k)$ is the reference trajectory, and $\Delta u(k|t)$ is the control increment; N_p and N_c represent the prediction time domain and control time domain respectively, and Q and R are the weight matrices. This objective function not only constrains the deviation of the target trajectory from the coverage rate, nucleation density and defect trend, but also suppresses the drastic jumps in the control quantity, avoiding the reverse interference caused by frequent oscillations of the heating power and flow command on the growth stability.

Considering that the solution of MPC depends on state prediction, this paper uses a discrete state space model to describe the growth process of graphene:

$$x(t+1) = Ax(t) + Bu(t), y(t) = Cx(t) \quad (7)$$

In the equation, $x(t)$ represents the state vector, $u(t)$ is the control input, $y(t)$ is the output vector, and A , B , and C are the system matrices identified from the process data. To ensure that the control result conforms to the operating boundaries of the equipment, additional hard constraints need to be added:

$$u_{\min} \leq u(t) \leq u_{\max}, y_{\min} \leq y(t) \leq y_{\max} \quad (8)$$

This means that the heating power, gas flow rate and pressure adjustment amount must always remain within the allowable range of the actuator, and the output such as coverage and temperature must not exceed the process safety boundaries. For short-term tolerable minor

deviations, the controller introduces penalty terms in the computer solution module for gradual mitigation, to balance convergence speed and response flexibility.

In terms of specific implementation, the MPC optimizer is deployed in the upper-level software, and the sampled data is cached, synchronized and updated before being sent to the solver to obtain the future control sequence, but only the first control quantity of the current moment is executed; when the next sampling moment arrives, it will re-predict and correct based on the new state. This rolling time-domain strategy can continuously absorb the latest process information and weaken the influence of model mismatch and external disturbances. Considering that the solution of multi-variable constraints has certain computational pressure, this paper adopts a fast quadratic programming solution method in the program design and limits the number of single-cycle iterations to ensure that the control instructions can be output within the set sampling time. The resulting "collection - prediction - optimization - execution" closed-loop algorithm provides a direct control basis for the subsequent online adjustment of growth parameters, stability analysis and disturbance robustness verification.

2.4 Closed-loop Regulation Mechanism of Growth Process and Computer Implementation

The key to the closed-loop regulation of the growth process of graphene nanostructures lies not in the issuance of a single control instruction, but in organizing the reaction chamber, sensor acquisition, state estimation, iterative optimization, and execution feedback into a continuous and iterative unified chain. Based on this, this paper constructs a closed-loop mechanism of "perception - transmission - prediction - decision - execution - correction" in the computer control system. During the growth process, temperature, pressure, methane flow rate, hydrogen flow rate, and in-situ surface signals are collected in real time by sensor nodes, and sent to the upper computer through data acquisition card and serial port communication module. After the upper computer completes noise reduction, timestamp alignment, and outlier elimination, it writes the process data into the state update module, which is used to generate the current state vector $x(t)$ at the current time.

On this basis, the MPC solver generates control instruction sequences based on the identified state space model and the reference growth trajectory. If the control output at time t is represented as

$$u_t = \{u_T(t), u_C(t), u_H(t), u_P(t)\} \quad (9)$$

Among them, $u_T(t)$, $u_C(t)$, $u_H(t)$ and $u_P(t)$ correspond to the heating power, methane flow rate, hydrogen flow rate and pressure regulation quantity respectively. The solver only executes the first control quantity of the current cycle, and the remaining parts are left to be recalculated in the next sampling cycle. This "predict a section, execute one step" approach enables the controller to continuously absorb the latest process information and avoid parameter setting lagging behind the changes in the growth state.

After the control instructions are sent through the communication interface to the heating unit, mass flow controller and pressure regulating valve, each executing component returns the actual execution result and status feedback, forming a feedback vector.

$$F(t) = \{f_1(t), f_2(t), \dots, f_m(t)\} \quad (10)$$

The feedback information includes completion status of execution, current process parameters and deviation values, etc. The system compares the feedback state $x_r(t)$ with the predicted state $\hat{x}(t)$ of the model, and constructs the deviation term.

$$e(t) = x_r(t) - \hat{x}(t) \quad (11)$$

If $e(t)$ exceeds a certain range, the error compensation subsystem will update the state representation coefficients or prediction factors in an incremental manner to eliminate the accumulation of errors caused by model mismatch, sensor element drift, and external disturbances.

The upper-level machine scheduling program controls the closed-loop process at a fixed time interval. It implements the software layer operation in a multi-threaded mode, allocating tasks such as receiving data, state update actions, optimization algorithms, and issuing commands to different task queues to improve response speed and reduce module blocking risks. Since it is a closed-loop regulation, monitoring the growth state of graphene, adjusting parameters, and correcting feedback on the same computer not only speeds up our control feedback but also provides an experimental basis for subsequent stability analysis and robustness analysis.

3 Experimental System and Verification Environment Construction

3.1 Configuration of Graphene Growth Experimental Platform and Computer Control System

To ensure the stability of the graphene growth process and the requirements for long-term data collection and command issuance, the reactor and the computer control module are integrated in a single design. The core instrument of the CVD graphene growth generator is the main component, consisting of a temperature control system, an air supply system, a pressure system, and an on-site observation system. All of these are equipped with sensors and effectors. Moreover, all the information is operated through the central controller, such as receiving information, refreshing the status, solving the problem using the MPC algorithm and providing the answer. As described in Table 3, the system structure consists of five modules: the stress response module, the data collection module, the communication module, the computing control module, and the data analysis module. The connections between these modules are achieved through serial interface buses and industrial Ethernet, ensuring that sampling, calculation, and execution are completed within the same time period, maintaining the consistency of the entire graphene production process, and providing a reliable hardware and software foundation for subsequent simulation comparisons, parameter adjustments, and stability tests.

Table 3: Configuration of Graphene Growth Experimental Platform and Computer Control System

Module Category	Main Configuration	Hardware/Software Environment	Functional Description
Growth Reaction Module	Tubular CVD reactor, quartz chamber	Heating furnace, vacuum pump, gas supply system	Performs graphene growth reactions and provides process support
Data Acquisition Module	Temperature, pressure, and flow acquisition	Thermocouples, pressure sensors, flow meters	Collects real-time state data during the growth process
Communication Module	100 Mbps transmission rate	Industrial Ethernet, serial interface	Enables data communication between equipment and the host computer
Control Computing Module	Multi-core processor, 16 GB memory	MATLAB/Python	Executes state updating and the MPC optimization algorithm
Software Analysis Module	Graphical interface and database	Host computer monitoring program	Performs display, storage, alarm, and feedback control

3.2 Simulation Environment and Parameter Settings

To verify the applicability of the established model and control algorithm under different operating conditions, this paper has constructed a simulation environment corresponding to the actual CVD growth device on the computer, and used it as a parallel verification system for the experimental platform. The simulation module is based on the state space model and is implemented in the MATLAB/Simulink environment to achieve dynamic coupling calculations of temperature, pressure, gas flow rate and surface growth state. At the same time, Python programs are used to complete parameter invocation, data caching and result output, ensuring the consistency of model calculation, control solution and data recording. The simulation time step is set to 1 second, and the control cycle is consistent with the sampling cycle of the experimental platform to ensure that the virtual calculation process can be compared with the physical process in terms of timing.

In terms of parameter settings, based on the typical process range of graphene growth, the temperature setting value, methane and hydrogen flow rate, chamber pressure and initial coverage rate are grouped and input. During the simulation, small random perturbations are introduced to test the model's response ability to process fluctuations. At the same time, the system also sets a reference growth trajectory and constraint boundaries, enabling the MPC solver to complete rolling optimization within a limited prediction time domain. This simulation environment retains the main dynamic characteristics of the graphene growth process and provides repeatable and traceable verification conditions for subsequent experimental results comparison and stability analysis.

3.3 Implementation of Data Acquisition, Transmission and Feedback Control Process

To ensure a continuous connection between state recognition, parameter optimization, and control execution in the graphene growth experiment, this paper has constructed a complete data acquisition, transmission, and feedback control process in the experimental platform, and

unified the reaction device side and the computer control side to the same operating rhythm. The entire process is divided into five steps: sensor acquisition, data preprocessing, state update, optimization solution, and execution feedback. Temperature, pressure, methane flow rate, hydrogen flow rate, and in-situ monitoring signals are obtained in real time by on-site sensing nodes, sent to the upper computer cache area through the acquisition card, and then filtered, abnormal values eliminated, and timestamp aligned. Finally, they are written into the state update module. Based on the updated time series data after synchronization, the control software generates the current state vector and calls the mpc solver to obtain the parameter adjustment command at that time point; then, through the communication module, the obtained parameter adjustment command is sent to the corresponding heating subsystem, mass flow valve, and pressure regulating valve for real-time control.

To illustrate the relationship between each stage, we summarize the key elements of the step nodes as shown in Table 4. From Table 4, we can see the information required by each step point, the parameters that need to be changed, and the feedback lag time. It can be seen that the initial stage mainly involves capturing the process state, the intermediate stage mainly involves data conversion and calculation decisions, and the last three steps involve executing instructions and feedback results. These three steps are not isolated; they are connected in a circular loop through serial port communication and industrial control network, enabling model prediction, parameter adjustment, and practical feedback to be completed within a single sampling period, thereby avoiding control deviations caused by information lag. The design of this process establishes a unified data foundation and operation platform for subsequent growth process monitoring, stress response analysis, and comparative experiments.

Table 4: Configuration of Data Acquisition, Transmission and Feedback Control Process Nodes

Process Node ID	Process Stage	State Acquisition Parameters	Control Variables / Processing Content	Feedback Delay / s
F01	Sensor Acquisition	Temperature, pressure, CH ₄ flow rate, H ₂ flow rate	Raw signal reading	0.18
F02	Data Preprocessing	Timestamps, fluctuation noise, outliers	Filtering, synchronization, normalization	0.24
F03	State Update	Coverage estimation, nucleation density, defect trend	State vector generation	0.31
F04	Optimization Solution	Current state, reference trajectory, constraint boundaries	MPC rolling calculation	0.42
F05	Execution Feedback	Actual temperature, actual flow rate, valve status	Command return and deviation correction	0.27

4 Result Analysis

4.1 Tracking of Growth State and Model Fitting Accuracy Analysis

To verify the descriptive capability of the model established in this paper for the formation process of graphene nanostructures, five important state variables were selected, namely temperature values, container internal pressure, coverage rate, initial particle number, and

defect rate. The real-time collected results from the upper computer are compared with the model output, and error statistics and fitting evaluation are completed in the MATLAB environment. As shown in Table 5, the tracking effect of the model on temperature and pressure is relatively stable, indicating that the state update mechanism based on sensor data can accurately reflect the fluctuations of the underlying process. The fitting results of coverage and nucleation density also maintain a high degree of consistency, indicating that the model has a good representation ability for the surface growth evolution trend. In contrast, the error of defect characterization quantity is slightly higher, which is related to the presence of local noise in the in-situ signal and the lag in defect formation. From the overall results, the average relative error of each variable is controlled within 5%, and the fitting goodness is higher than 0.93. This indicates that the state space model established in this paper can retain the main dynamic characteristics of the graphene growth process while ensuring computational efficiency. This result also shows that the aforementioned data synchronization, feature mapping, and online correction mechanisms are effective, providing a reliable state basis for subsequent dynamic parameter optimization and stability analysis.

Table 5: Analysis of Growth Status Tracking and Model Fitting Accuracy

State Variable	Mean Absolute Error (MAE)	Mean Absolute Percentage Error (MAPE) / %	Goodness of Fit (R ²)
Temperature	4.2 °C	0.42	0.982
Pressure	0.009 kPa	1.74	0.976
Surface Coverage	0.028	3.12	0.958
Nucleation Density	$0.17 \times 10^8 \text{ cm}^{-2}$	3.86	0.944
Defect Characterization Index	0.031	4.57	0.931

4.2 Analysis of Dynamic Optimization Response Capability of Growth Parameters

To test the dynamic adjustment capability of the proposed model predictive control strategy in the growth process of graphene nanostructures, this paper conducted 10 consecutive control tests on a unified experimental platform, comparing the MPC method with the conventional fixed-formula control method, and simultaneously recording two indicators: parameter response delay and target recovery time. The parameter response delay refers to the time elapsed from the upper computer identifying the state deviation to the execution mechanism completing effective regulation; the target recovery time represents the time required for key variables such as temperature, flow rate, and pressure to return to the allowable fluctuation range after deviating from the reference trajectory. Both methods were operated under the same sampling period, the same disturbance amplitude, and the same initial conditions to ensure the consistency of the comparison results.

As shown in Figure 2, the parameter response delay under MPC control remains at a relatively low level overall. The 10 test results range from 0.71 to 0.76 seconds, with an average of 0.735 seconds and a maximum of only 0.76 seconds; while the response delay of the fixed formula control method is concentrated between 1.18 and 1.31 seconds, with an average of 1.240 seconds. Compared with the latter, MPC on average shortened the response delay by 0.505 seconds, a reduction of approximately 40.7%. This result indicates that the rolling prediction and online solution mechanism can quickly identify the current deviation and generate new control quantities, thereby reducing the state accumulation error caused by control lag.

From the perspective of target recovery time, the MPC method also demonstrates better dynamic adjustment capability. In the 10 rounds of tests, the recovery time under MPC control was stable between 2.35 and 2.44 seconds, with an average of 2.395 seconds and a fluctuation of only 0.09 seconds; while the recovery time of the fixed formula control was 3.47 to 3.76 seconds, with an average of 3.610 seconds and a fluctuation of 0.29 seconds. Compared with the average reset time of 1.215 seconds for the former, it has been shortened by approximately 33.7%, indicating that MPC can quickly restore the system to the reference trajectory neighborhood after encountering high-temperature impacts, airflow disturbances, and cabin pressure offsets, and the control effect between adjacent several rounds is relatively uniform, without the occurrence of a relatively severe long-tail recovery phenomenon.

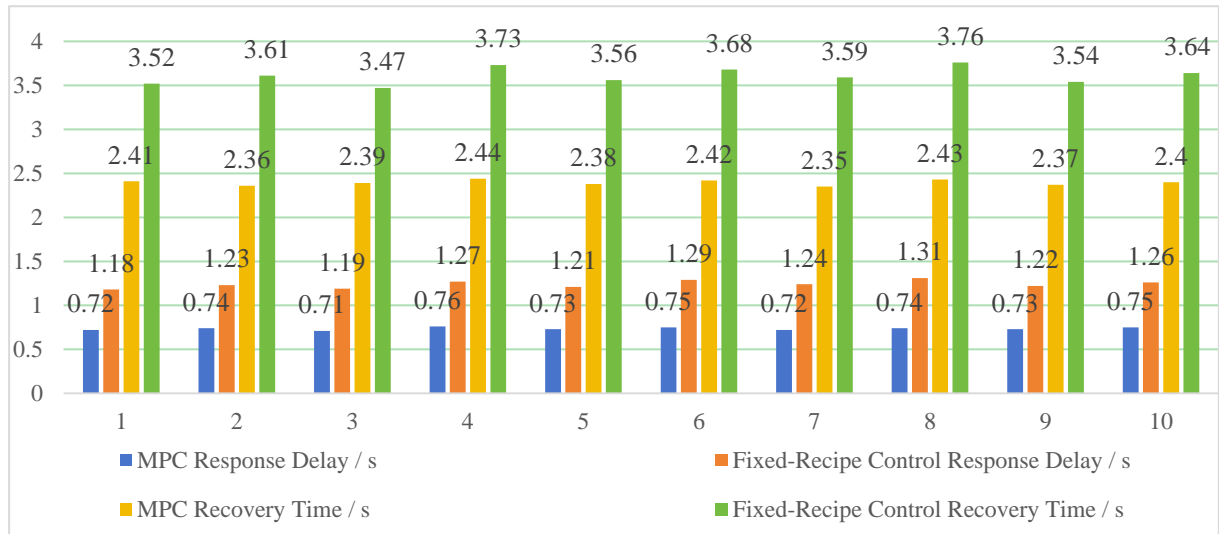


Figure 2: Comparison of Dynamic Optimization Response Capability of Growth Parameters

From the task log of the upper-level system, it can be found that under the fixed formula strategy, the response time and recovery time in the fourth, sixth, and eighth cycles have significantly increased. Especially in the eighth cycle, the response time is 1.31 seconds and the recovery time is 3.76 seconds, indicating that this strategy is very sensitive to various disturbances; while under the MPC strategy, these links still remain stable. They are 0.74 to 0.76 seconds and 2.42 to 2.44 seconds respectively, and this method has been verified to have higher stability and flexibility in feedforward regulation. Overall, the parameter dynamic optimization method based on MPC shows a faster response speed and more stable recovery ability during graphene growth, and can better adapt to complex conditions such as thermal field fluctuations, atmosphere disturbances, and execution delays, providing a more reliable control basis for subsequent consistency verification and stability analysis.

4.3 Verification of Consistency between Simulation Results and Experimental Results

To verify the consistency between the virtual prediction and the actual execution of the established model, this paper selects three key variables: temperature, chamber pressure, and methane flow rate. The output values of the simulation system and the measured values from the experimental platform are compared point by point at a unified sampling period, and synchronous plotting and error statistics are completed on the upper computer. These three types of variables correspond to the heat field regulation, chamber stability, and carbon source supply processes, and can more concentratedly reflect the degree of agreement between the

model's prediction results and the actual growth process. As shown in Figure 3, the simulation curves and the experimental curves maintain a high degree of consistency in the overall trend, and the turning points of the variable changes are basically synchronized. There is no obvious mismatch or long-term drift.

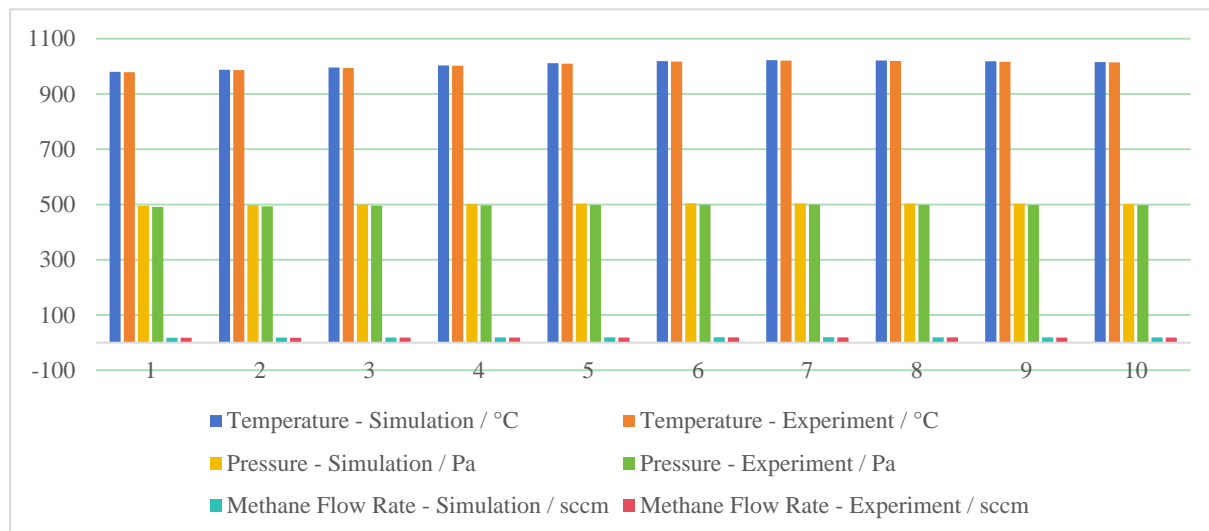


Figure 3: Comparison of consistency between simulation results and experimental results

From the specific data, at the 6th sampling moment, the simulated temperature was 1018.6°C, while the experimental temperature was 1016.9°C, with a difference of 1.7°C; the simulated pressure was 503.8 Pa, and the experimental value was 498.6 Pa, with a deviation of 5.2 Pa; the simulated methane flow rate was 19.4 sccm, and the measured value was 18.9 sccm, with a deviation of 0.5 sccm. At the 8th sampling moment, the temperature deviation decreased to 1.5°C, the pressure deviation was 4.6 Pa, and the flow rate deviation was 0.4 sccm. In terms of the overall statistical results, the average relative errors of the three variables (temperature, pressure, and flow rate) were 1.63%, 1.21%, and 2.08% respectively, indicating that the simulation model can accurately reproduce the state changes in the actual control process.

However, it should be noted that the minor errors mainly result from the thermal inertia of the physical device, the lag in valve response and the influence of the local environment. These do not indicate that there is a systematic deviation in our predictions of the system. Overall, the simulation system is quite close to the experimental results in terms of tracking trends, amplitude response and beat conversion. This indicates that the established model and the corresponding calculation process can be used for virtual mapping of steady-state characteristics and disturbance resistance tests in the future.

4.4 Analysis of Parameter Optimization Stability and Convergence Performance

To test the stability and convergence characteristics of the proposed method during the continuous growth process, this paper relies on the control logs of the upper computer and the operation records of the experimental platform. Five indicators, namely the standard deviation of temperature steady-state fluctuation, the standard deviation of pressure steady-state fluctuation, the convergence time of coverage deviation, the fluctuation amplitude of defect characterization quantity, and the control success rate, were selected for statistics. The MPC optimization strategy was compared with the fixed-formula control method. The relevant results are shown in Figure 4. Overall, under MPC control, all the indicators are superior to the

control method of comparison, indicating that this strategy not only can quickly correct the growth deviation but also can maintain a relatively stable operation state after parameter regression.

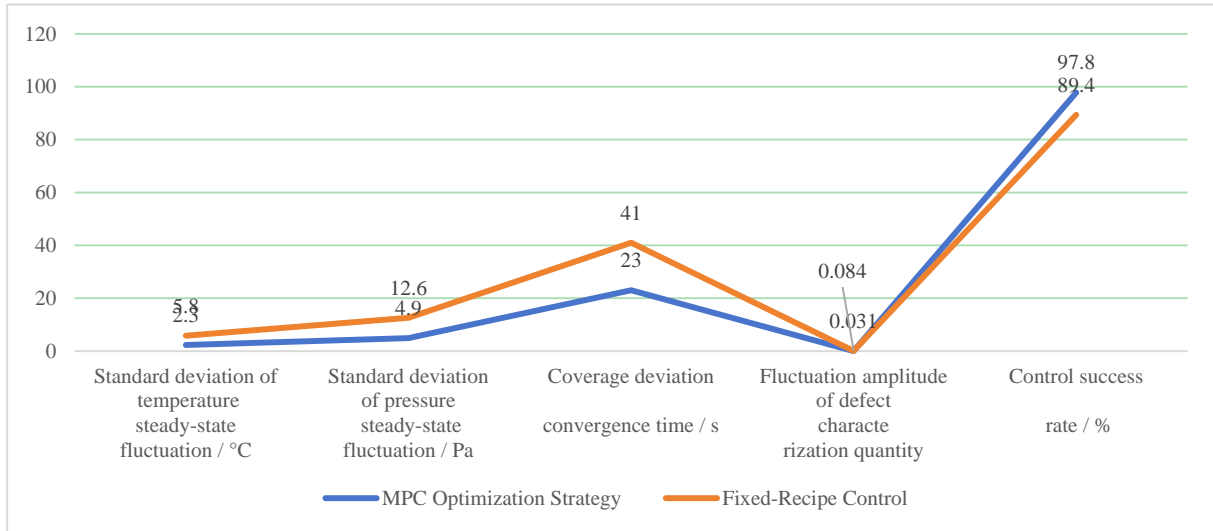


Figure 4: Comparison of stability and convergence performance of parameter optimization

From the perspective of steady-state fluctuations, the MPC method controlled the temperature standard deviation to 2.3 °C, which was 60.3% lower than the 5.8 °C controlled by the fixed formula; the pressure standard deviation decreased from 12.6 Pa to 4.9 Pa, a reduction of 61.1%. This indicates that under the combined effect of thermal inertia and gas transport, MPC can continuously compress the parameter fluctuation range through rolling optimization. In terms of convergence time for coverage deviation, MPC only took an average of 23 seconds, while the fixed formula control took 41 seconds, reducing by 18 seconds, a decrease of approximately 43.9%. The fluctuation amplitude of defect characterization quantities decreased from 0.084 to 0.031, indicating that after the intervention of closed-loop correction, local abnormalities will not continue to spread to subsequent growth stages. The control success rate also increased from 89.4% to 97.8%, reflecting the higher consistency of this method in multiple experiments.

By combining the iterative solution records on the computer end, it can be seen that MPC entered the stable convergence zone within the 6th to 8th control cycles, and the subsequent output increment significantly decreased, without continuous oscillation; while the fixed formula control often requires a longer adjustment time after disturbances, and there is a secondary offset phenomenon under local conditions. Thus, this method demonstrates better performance in terms of convergence speed, steady-state retention ability, and process consistency in parameter optimization, and can provide more stable control support for graphene nanoscale structure growth.

4.5 Robustness Verification of Growth Process under Disturbance Conditions

To test the adaptability of the proposed control method under complex working conditions, this paper sets up three typical disturbance scenarios in the computer control platform, namely temperature set value fluctuation, sensor noise interference, and short-term failure of the actuator unit. The average response delay, output deviation, and recovery time are recorded for these three indicators. The relevant results are shown in Figure 5. These three types of

disturbances correspond to the common thermal fluctuations in graphene CVD growth, the acquisition link noise, and the instantaneous abnormality of the flow actuator component, which can more comprehensively reflect the maintaining ability of the control system under non-ideal conditions.

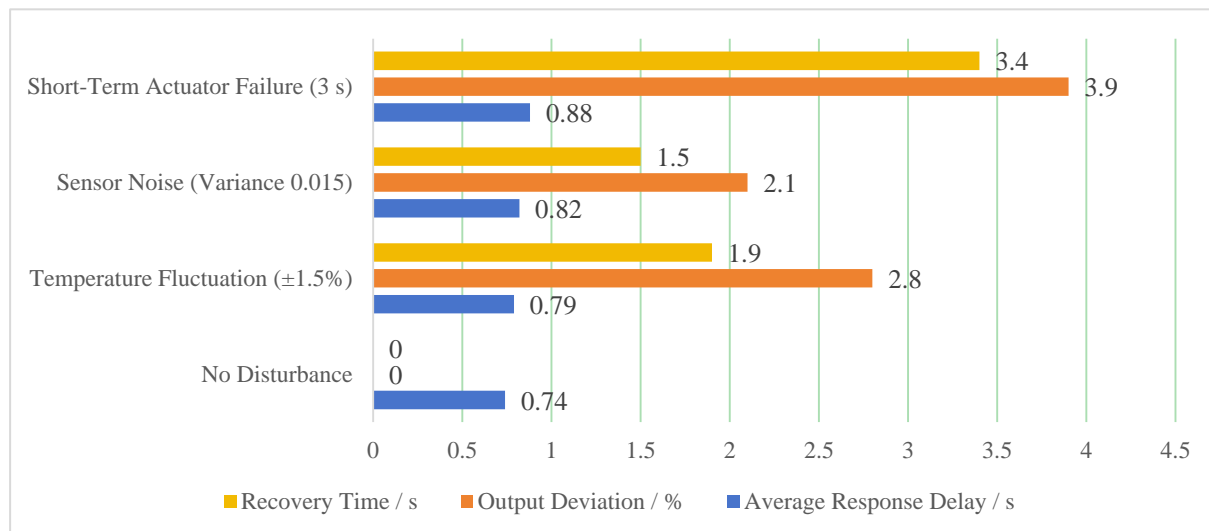


Figure 5: Verification results of robustness of growth process under disturbance conditions

From the test results, the average response delay of the system under no disturbance condition is 0.74 s; when the temperature set value fluctuates by $\pm 1.5\%$, the average response delay rises to 0.79 s, the output deviation is 2.8%, and the recovery time is 1.9 s. After adding Gaussian white noise with a variance of 0.015, the response delay is 0.82 s, the output deviation is 2.1%, and the recovery time is 1.5 s. This indicates that the state update module and filtering mechanism have a certain inhibitory effect on random disturbances. The short-term failure of the execution unit has the most significant impact on the system. Under the condition of short-term intermittent operation for 3 s, the average response delay increases to 0.88 s, the output deviation reaches 3.9%, and the recovery time is extended to 3.4 s. However, the control process does not show continuous oscillation or significant divergence.

By combining the log data of the upper computer, it can be seen that the MPC controller can quickly call the latest state vector to reconstruct the predicted trajectory and correct the temperature and flow instructions through rolling solution. Therefore, even in the abnormal scenario of the actuator, the system can recover to the allowable range within a relatively short time. Overall, the maximum delay increment under the three types of disturbances is only 0.14 s, and the maximum recovery time is 3.4 s. This indicates that the method proposed in this paper has good robustness and can provide a relatively stable dynamic correction capability for the growth process of graphene nanoscale structures.

4.6 Comparative Analysis with Existing Parameter Control Methods

To further illustrate the comprehensive advantages of the proposed MPC closed-loop optimization method in the control of the growth process of graphene nanostructures, in the same experimental platform, with the same sampling period and under the same disturbance conditions, this paper compared the proposed MPC closed-loop optimization method with fixed formula control, PID control, and local MPC control. Each method completed 10 consecutive growth regulation experiments, and the evaluation indicators included average response delay, deviation convergence time, steady-state error, and stability index. The relevant results are

shown in Table 6. Overall, the proposed method demonstrated better balance in all four indicators. Not only was the response faster, but the steady-state retention ability after dynamic correction was also more reliable.

Table 6: Performance Comparison of Different Parameter Control Methods

Control Method	Average Response Delay / s	Deviation Convergence Time / s	Steady-State Error / %	Stability Index
Fixed-Recipe Control	1.26	3.68	4.8	0.73
PID Control	0.98	3.14	3.5	0.81
Local MPC Control	0.86	2.79	2.6	0.88
Proposed Method	0.74	2.31	1.9	0.95

From the specific results, the average response delay of the fixed recipe control is 1.26 s, the PID control is reduced to 0.98 s, the local MPC is further shortened to 0.86 s, while the method proposed in this paper can be stably controlled at 0.74 s; compared with the fixed recipe control, the delay is shortened by 0.52 s, a reduction of 41.3%. In terms of deviation convergence time, the fixed recipe control and PID control are 3.68 s and 3.14 s respectively, while the local MPC is 2.79 s and the method proposed in this paper is 2.31 s, which is still shorter by 0.48 s compared to the local MPC. The steady-state error decreases from 4.8% of the fixed recipe control to 1.9% of this method, indicating that under the conditions of temperature, atmosphere and pressure coupling changes, this method tracks the target trajectory more tightly and has smaller parameter drift. In terms of stability index, this method reaches 0.95, which is higher than 0.88 of local MPC, 0.81 of PID control and 0.73 of fixed recipe control, indicating that its output fluctuations are smaller and the control results are more uniform in multiple rounds of experiments.

This difference is related to the control architecture. The fixed recipe control relies on preset process windows and can only passively withstand disturbances; the PID control has certain feedback capabilities but is limited in handling multi-variable coupling and constraint boundaries; the local MPC can improve the effect of single-loop regulation but is difficult to coordinate the parameter linkage throughout the growth process. This method, however, utilizes the state update, rolling prediction and online solution mechanism of the computer end, integrates temperature, flow rate, pressure and surface state into the same control framework, thus achieving better comprehensive effects in dynamic response, convergence speed and stable maintenance. Thus, it can be seen that for the parameter optimization of the graphene nanoscale growth process, relying solely on local correction is no longer able to meet the requirements of high consistency control, and introducing the full-process MPC closed-loop regulation is more practically valuable.

5 Discussion

The aforementioned results indicate that when model predictive control is introduced into the growth process of graphene nanostructures, the performance improvement does not manifest in a single indicator, but is reflected simultaneously in multiple aspects such as response speed, convergence efficiency, steady-state retention, and disturbance suppression. Experimental results show that the average response delay of the method in this paper is 0.74 s, significantly lower than 1.26 s of the fixed-formula control; the deviation convergence time is shortened to 2.31 s, and the steady-state error is reduced to 1.9%. Even under the condition of short-term failure of the execution unit, the system can recover to the allowable range within 3.4 s. This

demonstrates that the advantage of MPC is not just "responding faster", but lies in its ability to use the rolling prediction and online solution on the computer end to complete early correction before the deviation spreads, thereby compressing the amplification effect of thermal field fluctuations and atmosphere disturbances on the subsequent growth stage. Compared with PID control and local MPC methods, the improvement of this method also lies in the overall process coordination. Traditional feedback control pays more attention to the single-variable error feedback and is insufficient in considering the interaction between temperature, flow rate, pressure and surface state; local MPC can improve the dynamic regulation ability of a certain link, but is difficult to cover the continuous relationship between nucleation, expansion and defect evolution. This paper unifies the state acquisition, feature mapping, prediction calculation and control execution on the upper computer into the same closed-loop framework, so that the control decision no longer relies on single-point empirical judgment, but is based on the update of all process data. This is also the important reason for its stability index to reach 0.95.

Of course, this method still has certain limitations. On the one hand, the model accuracy is still affected by the quality of in-situ observation and the ability of state estimation, and the fitting error of defect characterization is relatively high, indicating that the complex microscopic changes have not been fully characterized. On the other hand, as the number of control variables and constraints increases, the computational burden of MPC online solution will also increase, and higher requirements are placed on the performance of the processor and communication stability. Further research can be carried out from two aspects: one is to introduce an adaptive prediction model more suitable for nonlinear growth processes to improve the characterization ability of complex surface evolution; the other is to combine reduced-order modeling and fast solution strategies to further compress the control cycle and enhance the method's portability in more complex process scenarios. Overall, the parameter optimization framework constructed in this paper provides a clearer implementation path for the stable control of the graphene nanostructure growth process. It not only improves the dynamic regulation quality of key parameters, but also provides a verifiable technical basis for computer participation in the control of material growth process.

6 Conclusion

This paper focuses on the issues such as strong parameter coupling, significant dynamic fluctuations, and difficult stable control during the growth process of graphene nanostructures. A parameter optimization and closed-loop control method based on model predictive control was constructed, and the state representation, rolling prediction, online solution, and execution feedback were unified into a computer control framework. The research results show that the established model can accurately represent key state variables such as temperature, pressure, and coverage rate, and the simulation results maintain a high degree of consistency with the experimental results. In the dynamic regulation experiment, the average response delay of the system was reduced to 0.74 s, the deviation convergence time was shortened to 2.31 s, the steady-state error was controlled within 1.9%, and the stability index was increased to 0.95, demonstrating good response speed and process maintaining ability. The disturbance test further indicates that this method still has strong recovery ability under conditions of temperature fluctuations, sensor noise, and short-term abnormality of the execution unit. The study shows that combining MPC with the real-time computer control system can effectively improve the parameter drift and control lag problems in the graphene growth process, providing a relatively feasible technical path for the controllable growth of nanostructures. Further research can be conducted around nonlinear state modeling and rapid solution strategies.

Author's Profile

Junpeng Xie was born in Jiangmen City, Guangdong, China, in 2000. He obtained a master's degree from the University of Manchester in the UK. He is currently working in Shanghai, China. His main research direction is nanometer materials.

References

- [1] Anisur M R, Raman R K S, Banerjee P C, et al. Review of the role of CVD growth parameters on graphene coating characteristics and the resulting corrosion resistance[J]. *Surface and Coatings Technology*, 2024, 487: 130934. <https://doi.org/10.1016/j.surfcoat.2024.130934>
- [2] Huang Z, Jun L I, JIANG Y. Current status and prospect of graphene growth by chemical vapor deposition[J]. *New Carbon Materials*, 2025, 40(3): 457-476. [https://doi.org/10.1016/S1872-5805\(25\)60991-7](https://doi.org/10.1016/S1872-5805(25)60991-7)
- [3] Deng B, Liu Z, Peng H. Toward mass production of CVD graphene films[J]. *Advanced Materials*, 2019, 31(9): 1800996. <https://doi.org/10.1002/adma.201800996>
- [4] Zhang J, Lin L, Jia K, et al. Controlled growth of single-crystal graphene films[J]. *Advanced Materials*, 2020, 32(1): 1903266. <https://doi.org/10.1002/adma.201903266>
- [5] Choi M, Baek J, Zeng H, et al. Toward high-quality graphene film growth by chemical vapor deposition system[J]. *Current Opinion in Solid State and Materials Science*, 2024, 31: 101176. <https://doi.org/10.1016/j.cossms.2024.101176>
- [6] Munoz R, Gómez-Aleixandre C. Review of CVD synthesis of graphene[J]. *Chemical Vapor Deposition*, 2013, 19(10-11-12): 297-322. <https://doi.org/10.1002/cvde.201300051>
- [7] Saeed M, Alshammari Y, Majeed S A, et al. Chemical vapour deposition of graphene—synthesis, characterisation, and applications: a review[J]. *Molecules*, 2020, 25(17): 3856. <https://doi.org/10.3390/molecules25173856>
- [8] Yan K A I, Fu L E I, Peng H, et al. Designed CVD growth of graphene via process engineering[J]. *Accounts of chemical research*, 2013, 46(10): 2263-2274. <https://doi.org/10.1021/ar400057n>
- [9] Yan Z, Peng Z, Tour J M. Chemical vapor deposition of graphene single crystals[J]. *Accounts of chemical research*, 2014, 47(4): 1327-1337. <https://doi.org/10.1021/ar4003043>
- [10] Kidambi P R, Ducati C, Dlubak B, et al. The parameter space of graphene chemical vapor deposition on polycrystalline Cu[J]. *The Journal of Physical Chemistry C*, 2012, 116(42): 22492-22501. <https://doi.org/10.1021/jp303597m>
- [11] Papon R, Pierlot C, Sharma S, et al. Optimization of CVD parameters for graphene synthesis through design of experiments[J]. *physica status solidi (b)*, 2017, 254(5):

1600629. <https://doi.org/10.1002/pssb.201600629>
- [12] Li Q, Luo J, Li Z, et al. Effect of growth conditions and reactor configuration on the growth uniformity of large-scale graphene by chemical vapor deposition[J]. *Journal of Vacuum Science & Technology A*, 2024, 42(3). <https://doi.org/10.1116/6.0003487>
- [13] Tsakonas C, Manikas A C, Andersen M, et al. In situ kinetic studies of CVD graphene growth by reflection spectroscopy[J]. *Chemical Engineering Journal*, 2021, 421: 129434. <https://doi.org/10.1016/j.cej.2021.129434>
- [14] Losurdo M, Giangregorio M M, Capezzuto P, et al. Graphene CVD growth on copper and nickel: role of hydrogen in kinetics and structure[J]. *Physical Chemistry Chemical Physics*, 2011, 13(46): 20836-20843. <https://doi.org/10.1039/C1CP22347J>
- [15] Zhang X, Wang L, Xin J, et al. Role of hydrogen in graphene chemical vapor deposition growth on a copper surface[J]. *Journal of the American Chemical Society*, 2014, 136(8): 3040-3047. <https://doi.org/10.1021/ja405499x>
- [16] Niu T, Zhou M, Zhang J, et al. Growth intermediates for CVD graphene on Cu (111): carbon clusters and defective graphene[J]. *Journal of the American Chemical Society*, 2013, 135(22): 8409-8414. <https://doi.org/10.1021/ja403583s>
- [17] Popov I, Bügel P, Kozłowska M, et al. Analytical model of CVD growth of graphene on Cu (111) surface[J]. *Nanomaterials*, 2022, 12(17): 2963. <https://doi.org/10.3390/nano12172963>
- [18] Yang B, Yang N, Zhao D, et al. Numerical simulation of graphene growth by chemical vapor deposition based on Tesla valve structure[J]. *Coatings*, 2023, 13(3): 564. <https://doi.org/10.3390/coatings13030564>
- [19] Eres G, Regmi M, Rouleau C M, et al. Cooperative island growth of large-area single-crystal graphene on copper using chemical vapor deposition[J]. *ACS nano*, 2014, 8(6): 5657-5669. <https://doi.org/10.1021/nn500209d>
- [20] Faulwasser T, Grüne L, Müller M A. Economic nonlinear model predictive control[J]. *Foundations and Trends® in Systems and Control*, 2018, 5(1): 1-98. <https://doi.org/10.1561/26000000014>